International Conference on Space Optics—ICSO 2020

Virtual Conference

30 March–2 April 2021

Edited by Bruno Cugny, Zoran Sodnik, and Nikos Karafolas

EUCLID's very large telescope ALIGNMENT

International Conference on Space Optics — ICSO 2020, edited by Bruno Cugny, Zoran Sodnik,
Nikos Karafolas, Proc. of SPIE Vol. 11852, 118522Z · © 2021 ESA and CNES
CCC code: 0277-786X/21/$21 · doi: 10.1117/12.2599461

EUCLID's very large telescope alignment.

Alexandre Gerbert-Gaillard, Wilfried Sommerer
Airbus Defence and Space SAS, 31 Avenue des Cosmonautes, 31 402 Toulouse, France

Euclid is a part of the European Space Agency Cosmic Vision Medium Class program. This mission's goal is to investigate the nature of dark energy, dark matter and gravity by observing the geometry of the Universe and the formation of structures over cosmological timescales.

Euclid Payload Module (PLM) includes a large TMA Korsch telescope in Silicon Carbide (SiC),, feeding a visible imager (VIS) and a near-infrared spectrometer and photometer (NISP). Both instruments are mounted at their respective focal plane position.

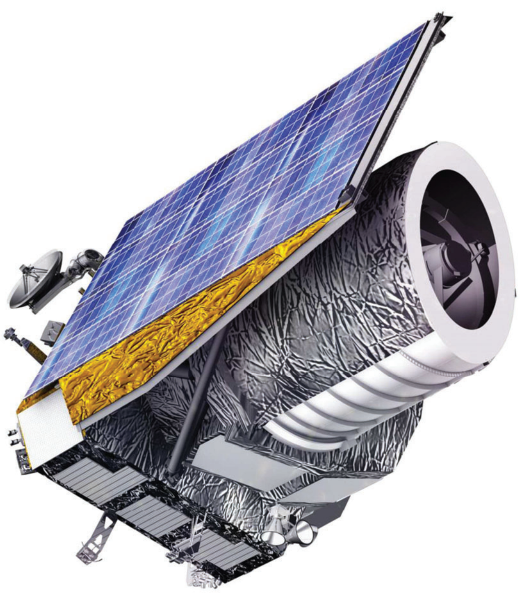

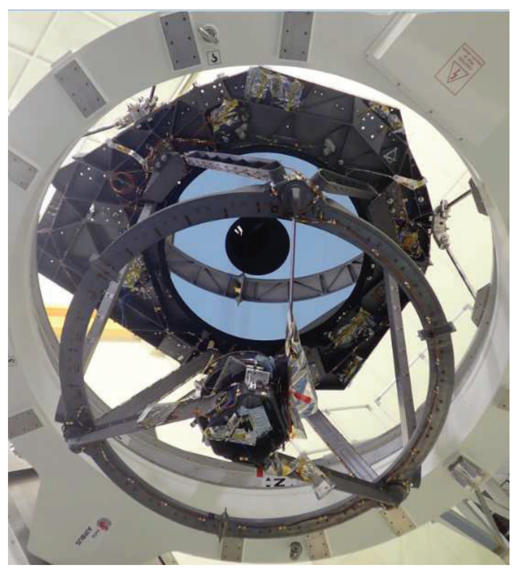

Figure 1. Artist's impression of Euclid satellite (credit ESA) Figure 2. PLM on integration trolley (credit Airbus)

Airbus Defence & Space, as main industrial responsible for the PLM design and assembly, has been in charge of the integration, the alignment and the optical performance characterization of this 7 mirrors telescope.

This paper describes how the alignment has been performed, with respect to the specified allocation for each mirror, and presents the performance results reached at the end of the alignment campaign.

Thanks to his long experience in making cutting edge, highly performant telescope, Airbus has successfully reached all the specified performance requirements, thus enabling its prime customer, Thalès Alenia Space, to finalize and complete the assembly of the whole satellite.

A 7 SIC mirrors telescope operating at 120K cold temperature.

The following picture illustrates the optical patch of the whole instrument: A 1.2m pupil diameter Korsch telescope is illuminating the 2 instruments, thanks to a specific dichroïc which separates the visible and infrared beams aimed by both instruments.

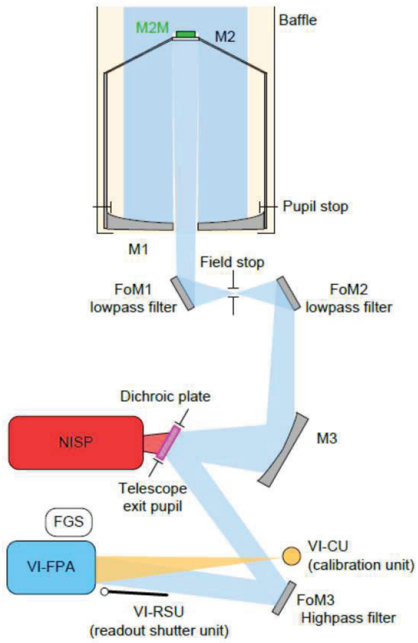

Figure 3. Payload Module scheme (credit Airbus)

Telescope type	Korsch
Focal length	24.5 m
Entrance pupil	Ø 1200 mm
M1	Ø 1250 mm
M2	Ø 350 mm
M3	535 x 406 mm²
FoM1	358 x 215 mm²
FoM2	283 x 229 mm²
FoM3	358 x 215 mm² (same as FoM1)
Dichroïc plate	Ø 117 mm
M1-M2 distance	1756 mm
Useful collecting area	1,006 m²
Offset	0.47°

Figure 4 : Main characteristics of Euclid mirrors

Thanks to our knowledge and large heritage of full SiC telescope behaviour at cold temperature, a predictive model of the telescope has been established, thus enabling an alignment of the telescope at ambient temperature.

Therefore, the guideline philosophy of the integration sequence was the following :

- Mechanical integration and pre-alignment of 5 mirrors among 7, basically the M1, FoM1, FoM2, dichroic and FoM3 mirrors.
- Perform optical alignment on key aspherical mirrors, thanks to WFE measurements at focal plane level. Thus, Zernike coefficients, especially coma, astigmatism and focus terms will be measured on several reference points of the focal planes.
- In addition to WFE alignment, additional optical activities ensures full knowledge of the performance along the whole optical path : among them are exit pupil position measurement, gap field stop check, real focal length measurement and PSF acquisition.

At the end, a **final performance of 55nm RMS** must be reached on all the focal plane, with differential focus between NISP and VIS focal planes not exceeding 18µm +/-10µm.

Clean room set up description

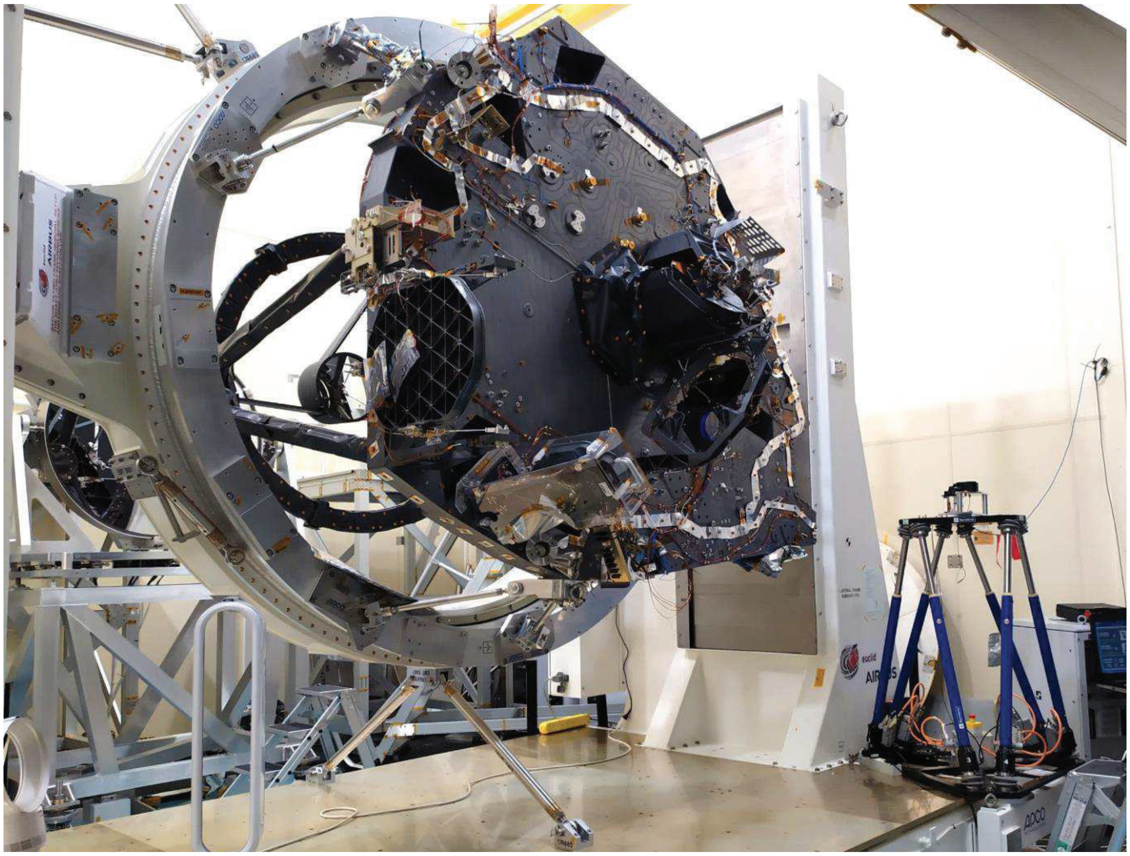

Figure 5. View of the ISO 5 clean room environment, with PLM on integration trolley, ready for WFE measurement (credit Airbus)

The alignment set up in ISO 5 clean room comprises an integration trolley, enabling on axis 180° rotation of the instrument, and a 1.3m reference AC Flat mirror located in front of the entrance pupil of the telescope. At the back of the PLM, a broadband wavefront sensor was mounted on a multi axis hexapod system, thus enabling to point at any reference location of the focal plane.

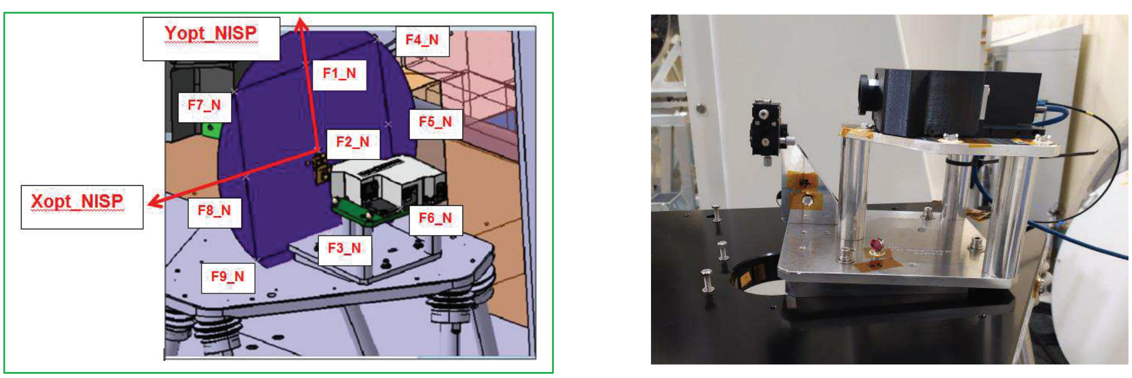

Figure 6. HASO wavefront sensor, with identified reference points of the NISP focal plane.

The so called “double path autocollimation set up” was feeded by an internal laser source, varying from 520nm to 1064nm wavelength.

Last but not least, all the set up was installed in a very stable ISO 5 clean room equipped with clean air laminar flux, anti-seismic floor and low variation thermal regulation.

Mechanical integration of mirrors

5 mirrors have been directly integrated on the PLM, using metrology data and MMT measurements performed at polisher level.

Stringent tolerances were specified. The goal was to have a first WFE of the telescope typically comprised between 500nm and 800nm, which was compatible with the wavefront sensor dynamic range.

Mirror	Translation tolerance, 3 axis (+/-,mm)	Rotation tolerance, 3 axis (+/-, mrad)
M1	0.2	0.15
FoM1	0.15	0.15
FoM2	0.15	0.15 in RX & RY, 0.3 in RZ
FoM3	0.15	0.15 in RX & RY, 0.3 in RZ
dichroïc	0.15	0.15 in RX & RY, 0.3 in RZ

Figure 7. Tolerances for the mechanical integration of the mirrors.

All the requirements regarding the mechanical integration have been reached, thanks to laser tacker measurements and operators skills, combined with specific in house MGSE tools manufactured in purpose to these AIT activities.

The final precision on the knowledge of the position of these mirrors is 50µm in translation and 50µrad in rotation.

WFE measurements

When it’s required to go down to a few nanometers RMS on the knowledge of the optical performance, you have to manage not only the telescope itself, but also its environment. It means, characterizing the Zernike coefficients variations, and if need be, find a way to reduce their amplitude.

As expected, and due to the very large size of this space telescope, the coefficients were quite disturbed when we performed the first series of measurements.

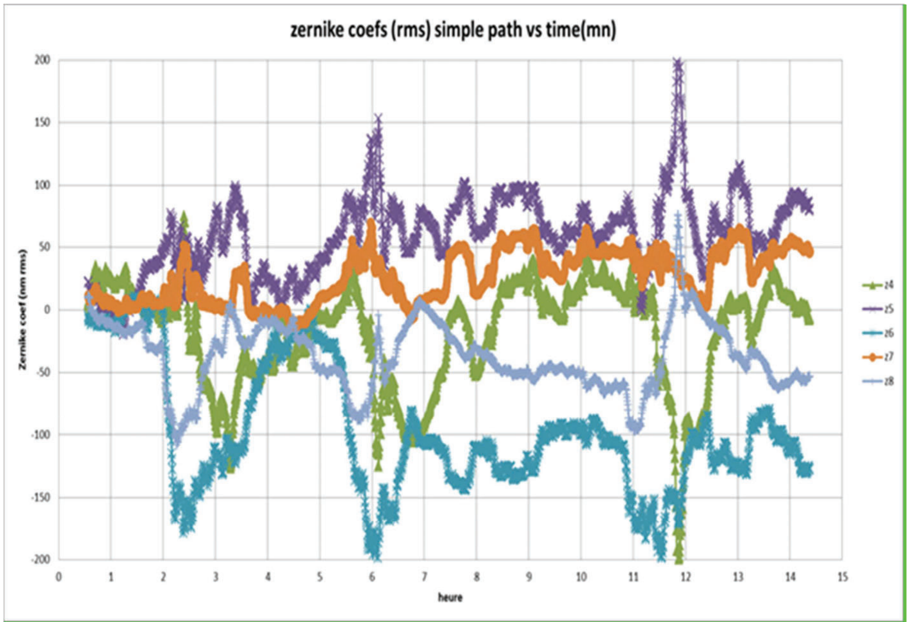

Figure 8. Recording of Zernike coefficient variations through the telescope.

Here is an illustration of this poor stability of the initial measurement. Zernike coefficients fluctuations are at very low frequencies which is a typical signature of air stratification.

The use more stringent temperature regulation, has lead to far better values, finally compatible with the precision target.

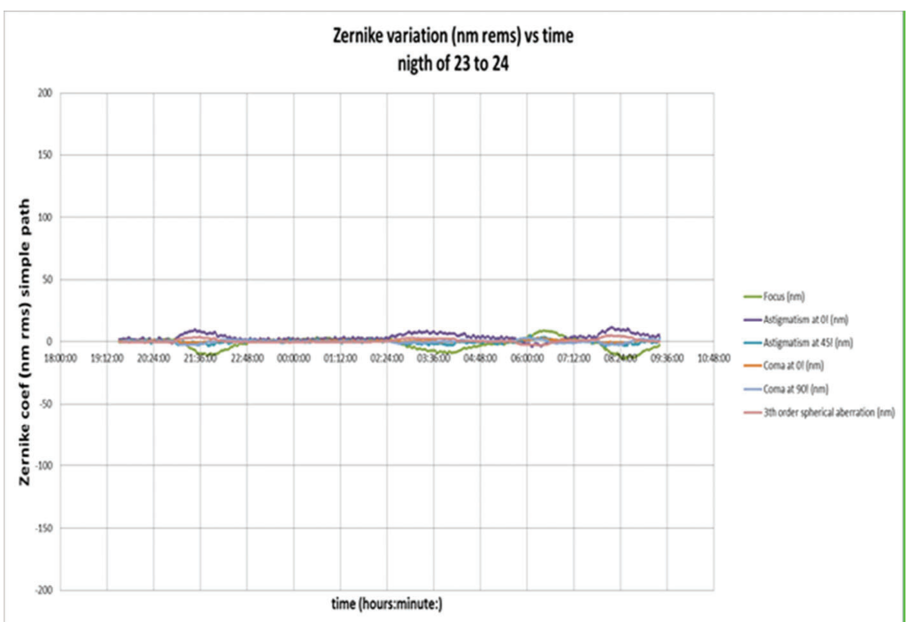

Figure 9. Recording of Zernike coefficient variations through the telescope, with improved environment control.

This ventilation configuration was therefore decided to be the nominal one for all alignment phases.

Once stability was achieved, a first WFE map was acquired at the center of the field, thus enabling to roughly realign the M2 mirror, based on coma and astigmatism Zernike values. Performance quickly goes from 500nm RMS down to a few hundred of nm RMS.

Then, the fine alignment requires to acquire data on several points of the field, as described on picture 6. This was quickly reached with the help of the hexapod, enabling repositioning of the wavefront sensor focal point to a few µm of the as design location.

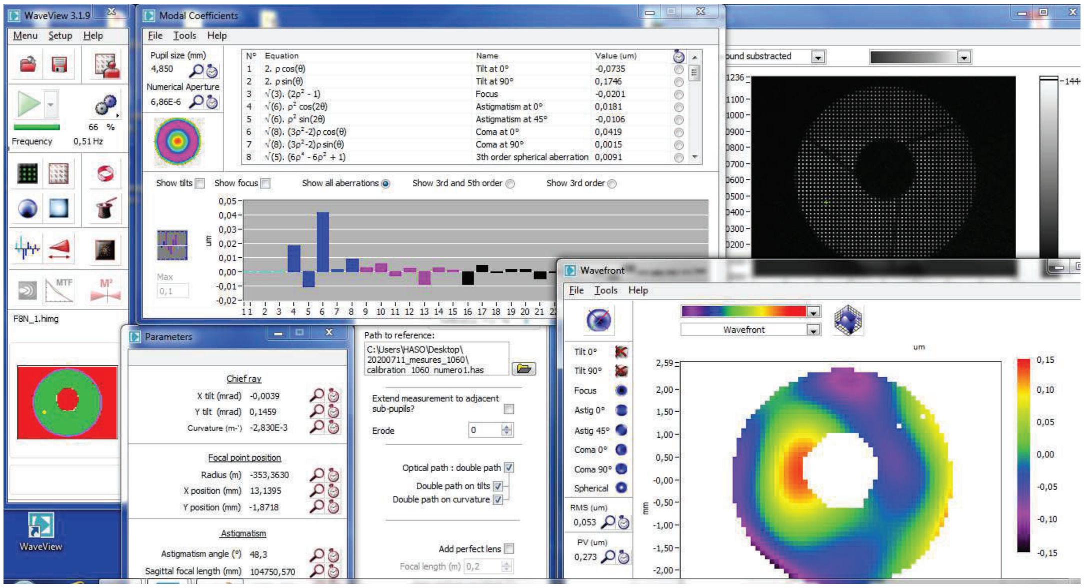

Figure 10. Typical WFE acquisition panel. Microlenses pupil, Zernike coefficient and reconstructed map are visible.

All the WFE values were integrated onto an in house alignment tool, giving optimisation corrections to be applied on M2 and M3 mirrors, on all 6 axis.

At this step, the performance reached a few dozen of nm RMS, but still not enough to be fully compliant.

To go even farther, it was necessary to take into account the gravity effect on the telescope behaviour. As the telescope is aligned on ground, it is necessary to compensate the gravity effect on the telescope, which is not present at the end once the telescope is operated in orbit.

A prediction model has been done, and compared to measurements with PLM rotated by 180°. At the end, the 0 G WFE performance was the sum of the 2 measurements +1 G and -1 G, divided by 2.

Finally, this last iteration on the correction of M2 and M3 mirrors leads to a final NISP WFE performance compliant with the specification of maximum 55nm RMS.

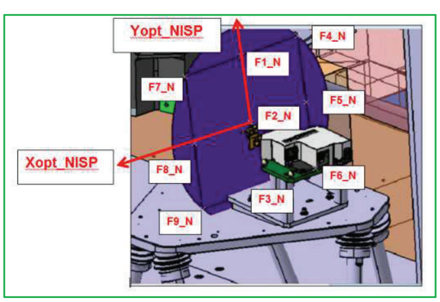

39	32	40
29	35	45
40	44	29

Figure 11. Final WFE RMS performance on NISP F1 to F9 reference points (in nm RMS).

Pupil centration

In addition to WFE performance measurements, several geometrical characteristics of the telescope were measured and checked.

One of them is the exit pupil centration, meaning the M1 entrance pupil seen from the focal plane. The position was measured in terms of lateral margin, compared to a mechanical baffle taken as a reference. Several pictures were taken, and then post processed to compute the margin expressed in mm.

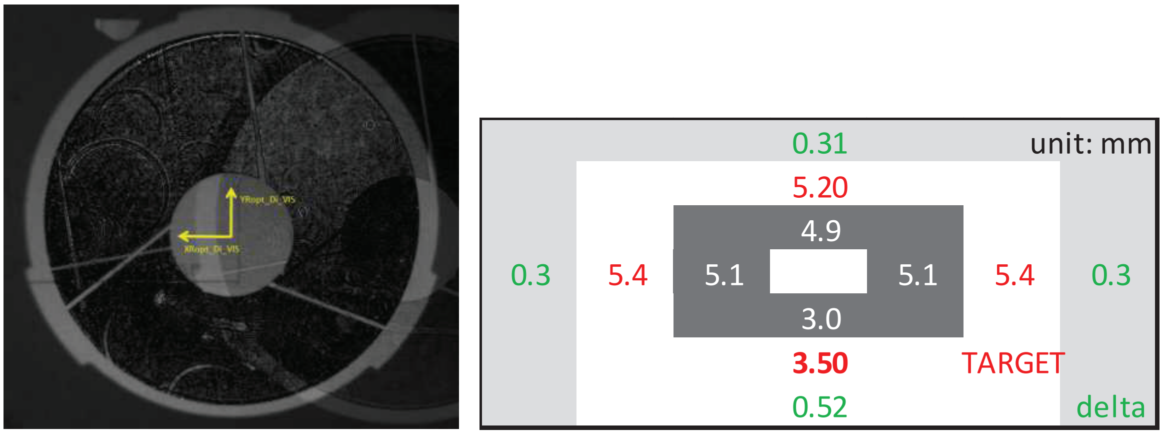

Figure 12. Pupil acquisition, and associated gap & variation with as design values.

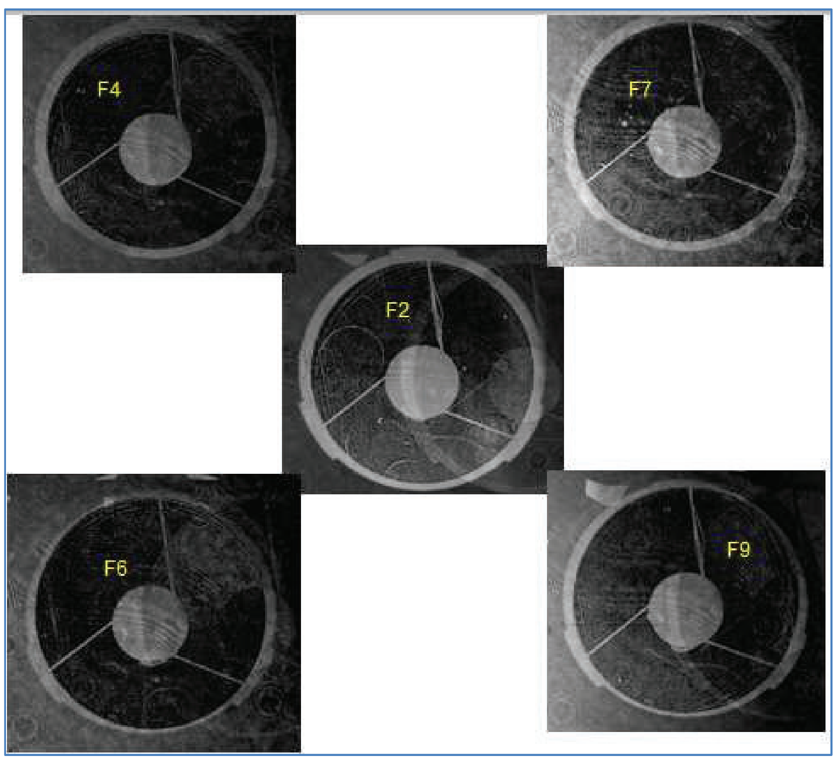

Figure 13. Pupil acquisitions at several reference points of the NISP focal plane.

Los instrument

Another geometrical check is the real focal length measurement. In this case, theodolites have been used for different autocollimation points. Measuring the LOS of the telescope on each point enables to reconstruct the on axis real focal length (RFL) of the instrument.

The measured focal length was 24730.9mm, for an as design value of 24742.1mm, meaning a deviation lower than 0,2%, thus compliant to the specification.

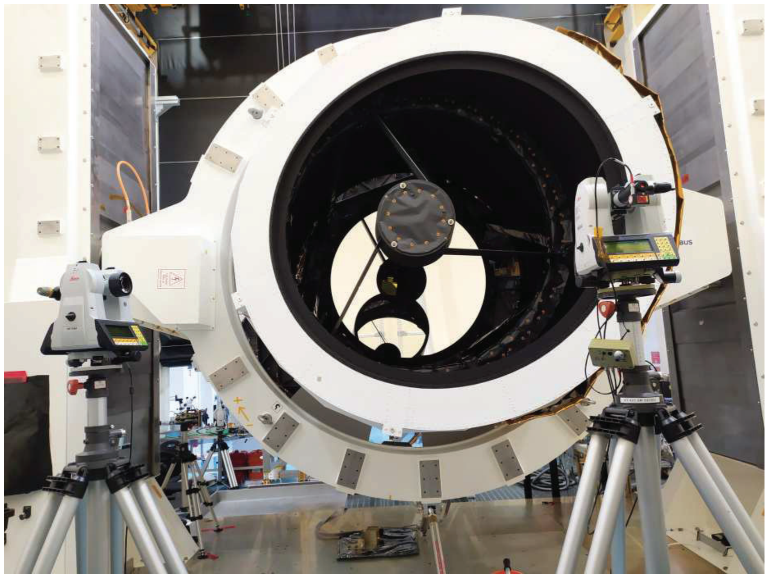

Figure 14. LOS measurement set up in ISO 5 clean room.

LOS Measurement expressed in GLOCV					IP measurement expressed in VIS FPA		
PRESENCE	LOS_ID	ux_GLOCV	uy_GLOCV	uz_GLOCV	FP_ID	X_VISFPA (mm)	Y_VISFPA (mm)
Y	LOS_1	0.000156883	-0.008298432	-0.999965555	FP_1	2.363532	157.774106
Y	LOS_2	0.000166625	-0.014693229	-0.999892035	FP_2	2.487223	0.144498
Y	LOS_3	0.000157366	-0.020995148	-0.999779565	FP_3	2.413651	-157.456564
Y	LOS_4	-0.006636718	-0.008299717	-0.999943533	FP_4	-164.315948	157.830442
Y	LOS_5	-0.006607936	-0.014676104	-0.999870465	FP_5	-164.290662	0.136835
Y	LOS_6	-0.006576889	-0.020972624	-0.999758418	FP_6	-164.33121	-157.439895
Y	LOS_7	0.006964497	-0.008306996	-0.999941243	FP_7	169.227528	157.780054
Y	LOS_8	0.006897809	-0.014676132	-0.999868507	FP_8	168.332438	0.223596
Y	LOS_9	0.006907177	-0.020978471	-0.999756068	FP_9	169.210077	-157.444718
N	LOS_10				FP_10		
N	LOS_11				FP_11		
N	LOS_12				FP_12		
N	LOS_13				FP_13		
N	LOS_14				FP_14		
N	LOS_15				FP_15		
N	LOS_16				FP_16		
N	LOS_17				FP_17		
N	LOS_18				FP_18		

	MEAS	AS DESIGNED	Delta		Criterion
X0(mm)	-1.6	0.0	-1.6	mm	
Y0 (mm)	361.413	352.861	8.552	mm	
PFL (mm)	-24471.4	-24497.0	-0.10%		
D	21.8	20.8	4.84%		
X0(mm)	-1.6	0.0	-1.6	mm	
Y0 (mm)	362.7	360.1	2.6	mm	
RFL 9PT VIS	-24730.9	-24742.1	-0,05%		0.2%

Figure 15. LOS measurement results and outputs.

Gap field stop

The field stop of the telescope is located between the FoM1 and the FoM2 mirrors, at the intermediate focal plane position. It is physically constituted by a physical window that traps any undesired light beam, taking into account a small margin gap with the useful optical beam.

As it was mechanically integrated at nominal position before mirror alignment, it was necessary to check the lateral gap between mechanical edge and optical useful beam.

This was performed by making pupil pictures acquisitions every 2mm all along the useful focal plane, thus scanning from internal to external the extinction of the light beam.

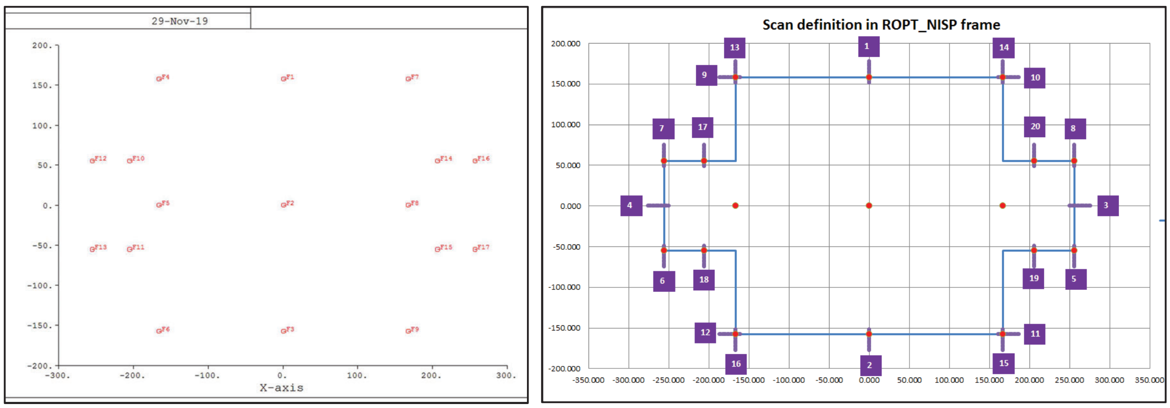

Figure 16. Full NISP reference points overview (LEFT), and associated scans locations (RIGHT).

We obtained galleries of pupil pictures showing the graduate extinction of the light beam, as it can be seen on the example below.

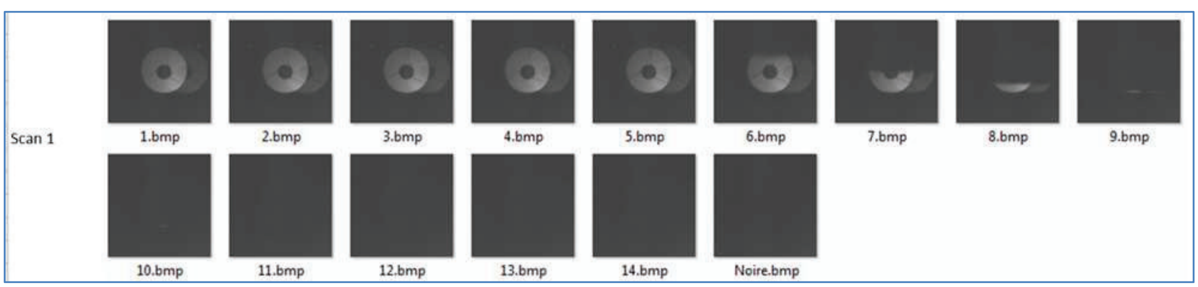

Figure 17. 2mm scan of pupil extinction (gap field stop measurement)

Finally, we extracted from these measurements the position of the camera where the extinction is at a level of 50% of the initial beam.

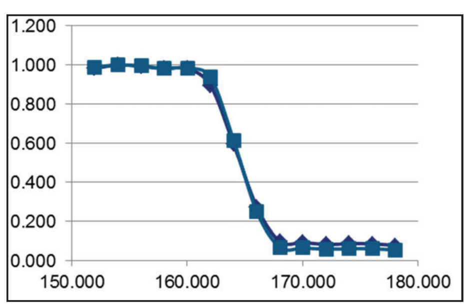

Figure 18. Light extinction curve computed from the acquisition scans

A comparison with the as-design theory has proven the appropriate integration and effect of the field stop, with final worst gap still lower than half of the allocation.

Chief ray vs edge at FS level	Meas. (mm)	As designed (mm)	Deviation (µm)
Scan 1 (F1)	6.97	7.14	-170
Scan 2 (F3)	9.48	9.55	-70
Scan 13 (F4)	6.82	6.67	150
Scan 16 (F6)	10.06	9.37	685
Scan 14 (F7)	6.8	6.67	130
Scan 15 (F9)	9.82	9.37	445
Scan 17 (F10)	6.67	6.21	460
Scan 18 (F11)	8.98	8.97	10
Scan 7 (F12)	6.5	5.98	520

Figure 19. Gap field stop results

All margins (VIS +NISP + FGS) are > 1,5 mm, and compliant with specification.

PSF

Another verification operated at ambient temperature is related to the PSF of a single source spot seen across the telescope.

For this measurement, a visible camera was implemented at the focal plane of the telescope, imaging the picture of a visible laser source.

The goal was to check the diffraction model of the PSF, as prediction shows a potential visible effect of the M1 quilting.

Several pictures were acquired, with different acquisition time, quick acquisition for unsaturated picture, and long exposure to visualise the diffraction figure of the PSF.

The result is the picture shown below, on which we can see both to the central spot and some diffraction points generated by the residual quilting effect of the M1.

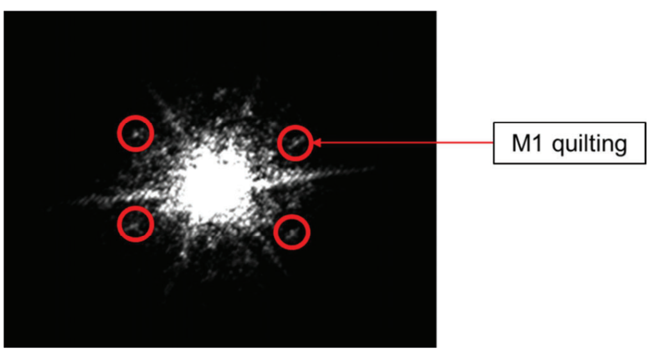

Figure 20. PSF at Euclid focal plane

The intensity between the central peak and the residual spikes is in a ratio of $1 * 10^{-6}$ factor, thus confirming the prediction model.

Differential focus

Last but not least, the most complex optical activity in terms of set up was the verification of the differential focus, in both optical channels, with a combined WFE measurement set up respectively implemented at the NISP and VS focal plane.

To do this, we performed a measurement bench with one wavefront sensor respectively mounted on NISP and VIS optical path, with both sensors pointing into the same combined line of sight of the telescope. This means getting a correlated position between the 2 focal planes.

The focusing point of the wavefront sensor system was finely characterised in terms of position, thanks to a laser tracker accurate to a few micrometers.

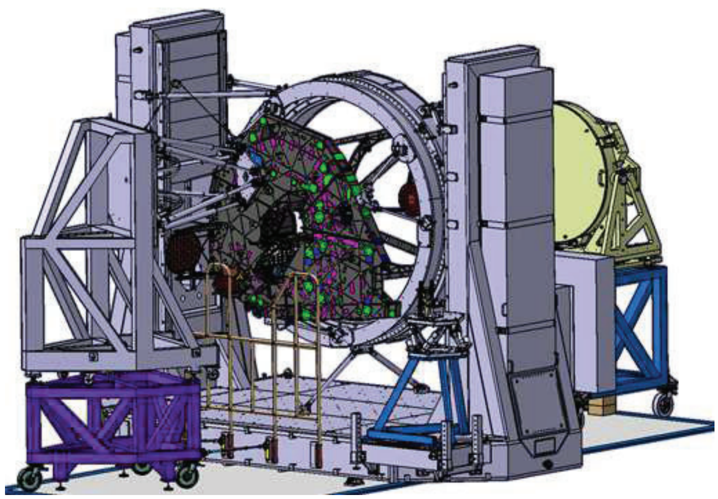

Figure 21. CAD viewe of the double WFE set up

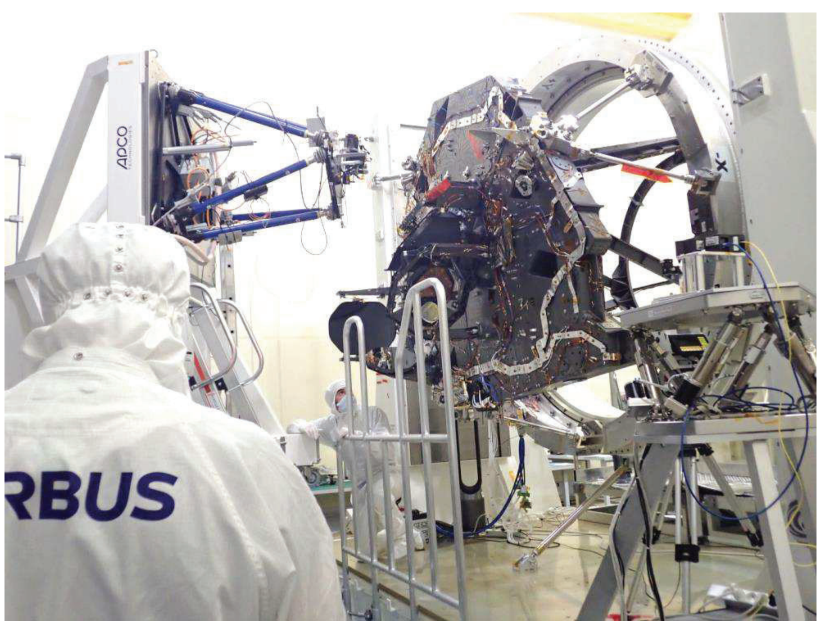

Figure 22. The same configuration, as really implemented in the clean room

Then, by performing combined WFE measurements, it was possible to check the focus correlation between the 2 optical paths. Remember: one telescope, but 2 focal planes, with no possible focus adjustment capacity at instrument level. Therefore, both have to be very precisely integrated, with a precision not exceeding a few dozen micrometers in between.

Measurement	Z4 (nm rms)	Target as designed (nm rms)	Delta (nm RMS)	Succes criterion
WFE (F2, NISP)	-3			
WFE (F2, VIS)	-27			
Differential Defocus (VIS – NISP)	-24	**-18**	6	10

Figure 23. Differential focus results

The measured differential defocus between VIS wrt NISP is -24 nm rms.

The success criterion of focus alignment accuracy of 10 nm RMS is achieved as Abs(-24- (-18))= 6 <10.

Conclusion :

Airbus, as industrial partner on side of ESA and TAS in the Euclid program, was in charge of the design, the manufacturing, the integration and the performance of the instrument, a cutting edge full SiC space telescope of 1.2m aperture.

Among all these activities, the alignment of the telescope, combined with multiple optical performance checks, have been successfully performed at Airbus Defence and Space Toulouse facility, bringing and establishing a new frontier in the capacity of producing very large optical space instruments.

Now the telescope is in its final sequence of integration in Airbus's clean room facilities in Toulouse, being prepared for critical mechanical and vacuum thermal tests, thus putting a final conclusion to the development of this extraordinary instrument.

Airbus wants to warmly thank the ESA team and the associated Euclid's scientific consortium, for their trust and their support all along the project, and also for simply making possible such kind of extraordinary project and challenge.

Airbus also wants to thank TAS Turin, as prime industrial customer and partner, for their respective cooperation and understanding all along the project.

Finally, Airbus is also grateful towards all the industrial partners who bring respective contribution to this project, thus emphasing the famous adage "*alone we go faster, together we go further*".